Development and Evaluation of an Ambulatory Stress Monitor Based on Wearable Sensors

Jongyoon Choi, *Student Member, IEEE*, Beena Ahmed, *Member, IEEE*, and Ricardo Gutierrez-Osuna, *Senior Member, IEEE*

***Abstract*—Chronic stress is endemic to modern society. However, as it is unfeasible for physicians to continuously monitor stress levels, its diagnosis is nontrivial. Wireless body sensor networks offer opportunities to ubiquitously detect and monitor mental stress levels, enabling improved diagnosis, and early treatment. This article describes the development of a wearable sensor platform to monitor a number of physiological correlates of mental stress. We discuss tradeoffs in both system design and sensor selection to balance information content and wearability. Using experimental signals collected from the wearable sensor, we describe a selected number of physiological features that show good correlation with mental stress. In particular, we propose a new spectral feature that estimates the balance of the autonomic nervous system by combining information from the power spectral density of respiration and heart rate variability. We validate the effectiveness of our approach on a binary discrimination problem when subjects are placed under two psychophysiological conditions: mental stress and relaxation. When used in a logistic regression model, our feature set is able to discriminate between these two mental states with a success rate of 81% across subjects.**

***Index Terms*—Electrodermal activity, heart rate variability, mental stress, wearable sensors.**

I. Introduction

STRESS is a term that describes bodily reactions to perceived physical or psychological threats [1]. Stress can be beneficial, keeping us alert in dangerous situations and focused to meet challenges. In most cases, however, stress is maladaptive and has detrimental health effects. As an example, stress is known to cause anxiety, fear, and is also a leading risk factor for heart-related diseases, diabetes, asthma, and depression. This makes stress management an important part of personal healthcare. However, it is impractical for us to maintain logs of changes in our stress levels throughout the day. Thus, a system that could monitor our stress levels over long periods, from weeks to months, would be invaluable. Access to this information would allow physicians to assess the effects of stress on our health and determine appropriate interventions.

Manuscript received April 15, 2011; revised August 22, 2011; accepted September 15, 2011. Date of publication September 29, 2011; date of current version March 7, 2012. This work was supported in part by the Qatar National Research Foundation under grant NPRP 08-125-2-031.

J. Choi and R. Gutierrez-Osuna are with the Department of Computer Science and Engineering, Texas A&M University, College Station, TX 77843 USA (e-mail: {rgutier, goonyong}@cse.tamu.edu).

B. Ahmed is with the Department of Electrical and Computer Engineering, Texas A&M University at Qatar, Education City, Doha, Qatar (e-mail: beena.ahmed@qatar.tamu.edu).

Color versions of one or more of the figures in this paper are available online at http://ieeexplore.ieee.org.

Digital Object Identifier 10.1109/TITB.2011.2169804

Advances in mobile computing and wearable sensors make it now possible to record a variety of physiological signals, as well as everything we see, hear, and do, on a twenty-four-hour basis. However, a wearable system suitable for long-term ambulatory monitoring must strike a balance between information content and comfort. Thus, the argument that "more sensors are better" is flawed, not only for statistical reasons [2] but also in terms of design for wearability [3]. Sensors must be carefully selected to measure variables that are relevant to the domain problem, and to do so without interfering with the users' daily activities. Here, we present a wearable sensor system that has been designed to meet the above criteria. The system can record a number of physiological variables known to be influenced by stress in an uninterrupted fashion for periods of more than thirteen hours.

The paper is organized as follows. Section II provides a brief background review of the relationship between stress and health, the known physiological correlates of stress, and prior work on wearable sensor platforms. Section III describes our wearable platform, from physiological sensors to hardware configuration and wireless communications. Section IV describes signal processing methods for our two primary sensing modalities (electrodermal activity and heart rate variability), proposes a new method for the analysis of heart rate variability that accounts for respiratory influences, and describes a stress prediction model based on logistic regression. Section V describes the experimental protocols used to elicit mental stress and relaxation. Experimental results are presented in Section VI, followed by conclusions and directions for future work.

II. Background

A. Stress and Health

Historically, stress has been defined as a reaction from a calm state to an excited state triggering a cascade of physiological reactions aimed at preserving the integrity of the individual [4]. Once the threat is averted, the body's physiological condition returns to normal. However, stress in modern life tends to be pervasive, as it arises mainly from psychological rather than physical threats. As physiological responses to stress are repeated over and over, the result can have adverse long-term effects on our health. Stress can be mental, emotional, or physical, making it difficult to assess.

If chronic, stress can have serious health consequences, e.g., elevated blood pressure can stimulate a thickening of the arterial walls, resulting in the blockage of blood flow through the narrowed arteries, potentially leading to a heart attack. Studies have linked work-related stress with an increased risk of

coronary heart disease [5], elevated ambulatory blood pressure [6], and an increased risk of myocardial infarction [1]. In the long-term, stress can damage the body as it results in suppression of the immune system [7], inhibition of the inflammatory response, increased blood pressure, damage to muscle tissue, infertility, and diabetes [8]. Suppression of the immune system leads to increased severity of the common cold [9] and increased susceptibility to infectious disease [10].

B. Physiological Variables for Mental Stress

Work over the past decade has seen human affective state monitored through speech, facial expressions, body gestures, and physiological variables [11]. Unlike speech and facial expressions, the response of physiological signals to emotions is hard to be controlled by individuals, hence they have been found to be more reliable in providing a "true" measure of the human emotional state [11], [12]. Due to the intense physiological reaction induced in the human body to the emotion of stress, physiological signals lend themselves best to stress monitoring. In this context, physiological monitoring using unobtrusive wearable sensors has been used to index stress and adjust the difficulty level of computer games accordingly [13], detect drivers' stress levels [14], identify early warning signs of work related stress [15], and remotely monitor patient's emotional state to provide to the healthcare provider [16].

A number of physiological markers of stress have been identified in the literature, including electrodermal activity, heart rate, various indices of heart rate variability, blood volume pressure, pupil dilation, electromyography, and respiration [17]. However, in order to gain acceptance as a method of stress management in a workplace and during activities of daily living, wearable sensors must be minimally cumbersome and inconspicuous, to avoid anxieties associated with wearing medical devices in public [18]. These usability considerations preclude some of the above measures from being considered as a long-term solution for stress monitoring. As an example, changes in blood volume can be monitored nonintrusively through photoplethysmography (PPG), but the sensors must be worn on a translucent part of the body (usually a fingertip or an earlobe), which interferes with daily activities. Another indicator of work stress, arterial blood pressure, is equally unsuited for long-term monitoring: accurate measurements are invasive (e.g., a needle must be inserted in an artery), whereas noninvasive methods (e.g., inflatable cuffs) are cumbersome, impractical, and inaccurate.

Fortunately, relatively simple and unobtrusive measures of inter-heartbeat intervals can provide a wealth of information about stress through the interaction between the heart and the autonomic nervous system (ANS). The ANS is composed of two main branches: the sympathetic nervous system (SNS) and the parasympathetic nervous system (PNS). The SNS branch increases heart rate and helps prepare the body for action in response to potential threats – the so-called "fight or flight" response. The PNS branch, on the other hand, reduces heart rate and is most active under unchallenging or relaxing situations, bringing the body back toward a rest state. PNS influences on heart rate, tends to occur at a much shorter time scale than SNS influences. Hence, by analyzing fluctuations in beat-to-beat periods, commonly referred to as heart rate variability (HRV) analysis, one can separate the contributions from both branches and infer stress levels.

Other minimally obtrusive sensing modalities include electrodermal activity (EDA), respiration, and electromyography (EMG). EDA is particularly advantageous for stress monitoring because the skin is exclusively innervated by SNS, whereas most other organs are under the influence of both autonomic branches. Thus, EDA is highly sensitive to emotional arousal (e.g., startle response, fear, anger) [19]. Respiratory signals also have diagnostic value: when stressed, respiratory rate increases, and breathing patterns become irregular. Finally, EMG can be used as an index of sustained stress by monitoring activity in the trapezius muscle [19].

C. System Considerations for Wearable Sensors

A number of wearable sensor systems have been developed over the past 15 years. In early systems, sensors were often wired into a data recording unit which was responsible for signal digitization and data storage. As an example, one of the best-known and pioneering systems (MIThril) [20] used wired physiological sensors connected to a Linux-based PDA. Wired connections are robust and reduce the need for separate power supplies, but the user must deal with dangling wires that hinder mobility. Alternatively, custom e-textiles have also been used to connect sensors [21], though this solution generally requires users to wear specially designed clothing.

A wide variety of technologies for wireless communication have become available over the past few years, from wide area networks (i.e., cellular) to short-range protocols (i.e., Bluetooth, ZigBee). Cellular networks may be used to transmit data to remote servers, and provide a high degree of freedom and mobility to the user. As an example, Anliker *et al*. [22] developed a wearable system to transmit electrocardiographic (ECG) and pulse oximetry data to a remote server using cell phones. However, cellular networks are too expensive to continuously transmit physiological data. Instead, various wearable sensor systems have used Bluetooth as an alternative communication protocol, since it can handle multiple sensors simultaneously. As an example, Mundt *et al*. [23] developed a wearable system for space and terrestrial applications that integrated ECG, impedance plethysmography, pulse oximetry, and body temperature, Bluetooth was used to transmit sensor signals to a data logger. Despite its ubiquity, Bluetooth has high-power requirements, which limit its usability to short experimental sessions (e.g., several hours) given the small power sources (i.e., coin-cell batteries) that must be used for usability reasons. Recently, the ZigBee protocol has become a popular alternative for wireless communication due to its power efficiency. As an example, Welsh and colleagues [24] developed an ad hoc network infrastructure for physiological sensors based on ZigBee motes (Micaz and Telos; XBow Inc.) Nonetheless, ZigBee was designed for field sensor network deployments, so it contains a number of functions that are not necessary for body-area-network applications. Instead, connection-based low-power

lightweight sensor network protocols (e.g., SimpliciTI; Texas Instruments Inc.) seem better suited for small RF networks.

Network topology is another important factor. One possible approach is for each sensor node to transmit data to a remote server through an ad hoc network. In iCalm, Fletcher *et al*. [16] used this approach to connect EDA and PPG sensors to a remote base station. This approach allows for smaller wearable sensors, but is impractical for ambulatory data collection since the sensor network must remain within reach of a remote base station. Therefore, the most logical configuration for ambulatory applications consists of having a body area hub that records data transmitted from various sensor nodes worn by the user. This configuration, known as a star topology, has been used in body sensor networks [25].

III. Description of the Wearable Sensor System

Having reviewed the various physiological correlates of stress and wearable technologies that may be used to monitor these signals, this section describes our design for a wearable sensor platform for stress monitoring in ambulatory settings.

A. Physiological Sensors

Several measurement techniques may be used to monitor heart rate variability. ECG is considered the gold standard but requires electrode wiring, which we deemed impractical for long-term use. HRV can also be estimated through pulse oximetry, but these measurements are very sensitive to motion artifacts. Instead, we decided to use a heart rate monitor (HRM) strap (Polar WearLink+; Polar Electro Inc.) that has gained wide acceptance for fitness monitoring.

Respiratory measurements are often neglected despite the fact that respiration has a dominant effect in heart rate variability. A number of sensing technologies can be used to capture breathing patterns. Respiratory inductive plethysmography (RIP) monitors change in thoracic or abdominal cross section by measuring changes in a magnetic field generated by coils embedded in a chest/abdominal strap. In impedance pneumography (IP), an alternating current is applied between two electrodes in the rib cage in order to measure impedance changes due to respiration. However, these sensors are sensitive to motion artifacts [26] and postural changes [27], which make them unsuitable for long-term ambulatory monitoring. Instead, we decided to employ a pressure-based respiration sensor (SA9311M; Thought Technology Ltd.) that proved robust to motion artifacts and could be integrated in the HRM strap for added comfort.

Changes in skin conductance (EDA) can be monitored by applying a low-level electrical voltage to the skin. Skin conductivity increases with sweat in response to stressors, so EDA is stronger in palms and fingers due to the higher density of eccrine sweat glands in those areas [28]. Although the palms are a good site for EDA monitoring, electrodes can be easily detached during ambulatory data collection. For this reason, we monitor EDA with two electrodes on the proximal phalange[1] of the index and middle finger (nondominant hand). Small AgCl electrodes (E243; In Vivo Metric Systems Corp.) are used for this purpose.

Finally, our system also includes a wireless surface-EMG module to monitor activation in the trapezius muscle. Namely, we place two snap lead AgCl electrodes (TDE205; Bio-Medical Instruments, Inc.) alongside the fibers of the trapezius muscle of the nondominant hand, and a third reference electrode near the acromion.

[1]As shown in Fig., placing the EDA electrodes in the proximal phalanges reduces interferences with normal activities (e.g., typing, grasping.)

B. Holster Unit

The holster unit consists of a data processing unit, a sensor hub, and a lithium-polymer battery. The holster unit measures $114 \times 50 \times 28$ mm, weighs 169 g, and provides data storage (2 GB mini SD flash), real-time signal processing, and ad hoc wireless networking. The system is an embedded Linux-centric platform based on a Verdex Pro motherboard (Marvell PXA270 400 MHz, 64 MB RAM; Gumstix, Inc.). The holster unit is connected to a sensor hub, which integrates a 3-D accelerometer (LIS344ALH; STMicroelectronics), a GPS unit (RXM-GPS-SR-B; Linx Technologies Inc.), and a real-time clock unit (DS1308; Dallas Semiconductor, Inc.). The sensor hub also contains an HRM receiver module (Polar RMCM01; Polar Electro Inc.), and a wireless transceiver (EZ430-RF2500; Texas Instruments Inc.) to communicate with the wireless sensors. The sensor hub is also responsible for power management of the holster unit; it contains a built-in charging module for a 3000 mAh Li-Po battery that allows continuous data collecting for over thirteen hours. After daily use, the subject can charge the holster unit overnight (6 h for a full charge) using a built-in charging circuit; a mini-B USB socket can be used to connect the holster unit to a power source (i.e., PC or iPhone-style wall charger). The charging circuit also protects the battery from over charging or under discharging.

On-board analog sensors (accelerometer and HRM receiver) are connected to an MSP430 microcontroller (Texas Instruments Inc.), where they are digitized and transmitted to the motherboard. RTC and GPS are directly connected to the motherboard through I2C and UART, respectively. The motherboard stores data onto a micro SD flash memory, and can also transfer the data to an external system via Bluetooth, though this option is only used sparingly to minimize power consumption. The building blocks of the wearable sensor architecture are shown in Fig. 1; an image of our current prototype is shown in Fig. 2.

C. Wireless Nodes

Each wireless sensor node contains a transceiver module (EZ430-RF2500; Texas Instruments Inc.). To date, respiration, EMG, and EDA sensors are ready to be used as wireless nodes. The wireless nodes are programmed for power efficiency; the wireless transmitter wakes up from sleep mode, captures a sample from the sensor, and goes back to sleep until the next data collection cycle. Data transmission is also done in an efficient manner; several samples are transmitted as a single packet to the sensor hub. The packet length and transmission rates are configurable. Average power consumptions are 10 mAh for the

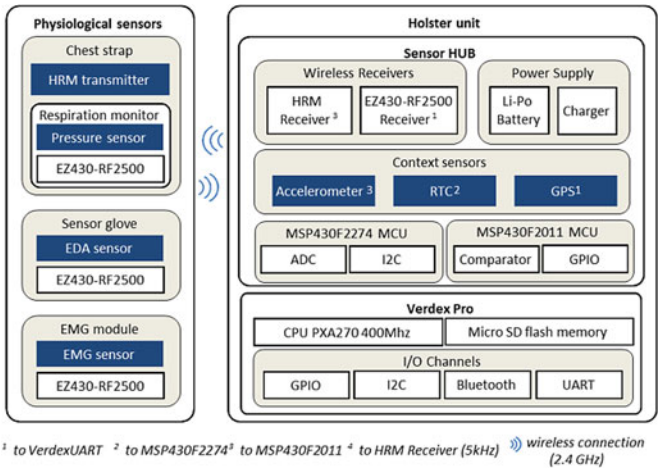

Fig. 1. Architecture of the wearable sensor platform. The holster unit integrates a sensor hub and an embedded-Linux motherboard. The sensor hub contains various context sensors and a 2.4 GHz transceiver that communicates with an array of wireless sensor modules. Each sensor module consists of a physiological sensor and wireless transmitter.

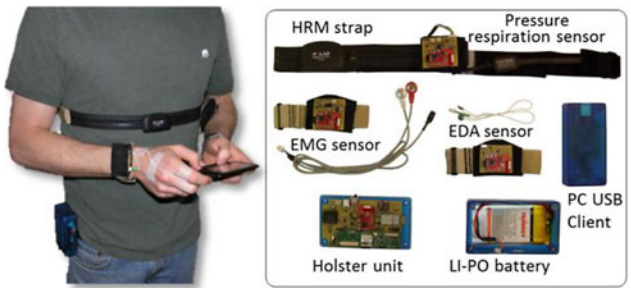

Fig. 2. Snapshot of a subject wearing the full sensor suite. The chest strap is shown outside the shirt for illustration purposes. The system consists of a holster unit, a chest strap combining HRM and respiration sensors, and wireless EMG and EDA modules. A USB transducer can be used to display sensor data in real-time on a PC monitor during sensor calibration.

EMG and respiration sensors, and 1 mAh for the EDA sensor. The sampling rate for respiration, EMG, and EDA sensors is programmable up to 300 Hz.

Wireless communications are based on SimpliciTI (Texas Instruments Inc.), a low-power lightweight sensor network protocol ideally suited for small RF networks. The network is configured in a star topology, where the sensor hub is the root and all sensor nodes are connected to the sensor hub as leaf node. Wireless transmission sometimes fails due to accidental power failures at the holster unit (e.g., the power is mistakenly turned OFF on the holster unit, and powered ON again). To prevent permanent disconnection, our communication implementation uses message acknowledgement (ACK) to increase the reliability of the wireless data transmission. When a wireless sensor node sends a packet to the holster unit, it requests an ACK. If the node fails to receive ACK from the sensor hub then it tries to re-send the packet for a predetermined number of times (i.e., default is five times) or until it receives ACK. If this preconfigured limit is exceeded, the node decides that the holster unit has experienced a power failure and the node attempts to establish a new connection. The reconnection procedure takes less than 3 s when the sensor hub is alive. After reconnection is established, the node continues to collect data from the sensor; any failed packets are lost and no data are collected during the reconnection procedure.

IV. Signal Processing Methods

A. Feature Extraction From Electrodermal Activity

The EDA response consists of two characteristic components: 1) a slowly changing offset known as the skin conductance level (SCL), and 2) a series of transient peaks known as skin conductance responses (SCR) [29] that occur in reaction to startle events (i.e., an unexpected loud noise) but also spontaneously, in which case they are referred to as nonspecific (NS-SCR). Several approaches have been proposed to decouple these two components. Lim *et al*. [30] proposed a curve-tting method with sigmoidal/exponential functions that decomposed EDA into discrete SCRs and the residual SCL. A related but computationally simpler approach was proposed by Alexander *et al*. [31] to decouple the two EDA components. The approach models the EDA time series as the convolution of an impulsive spike train, which controls the timing of SCRs, and a second-order differential equation, which controls the rise time and decay of individual SCRs (i.e., a biexponential function). Following [31], Benedek and Kaernbach [32] also modeled EDA as the result of a driver function (spike train) convolved with an impulse response. Since the driver function was assumed to represent sudomotor neuron activity (i.e., either spiking or at rest), the decomposition was performed by means of a non-negative deconvolution procedure. These methods can provide a fine decomposition into individual SCRs but tend to be computationally heavy and sometimes require manual inspection [31]. An alternative approach was proposed by Frantzidis *et al*. [33] to detect individual SCRs from the EDA derivative based on a peak-picking algorithm; the approach was also able to extract various SCR parameters (e.g., latency, rise time). Along these lines, in this study we use a regularized least-squares detrending method [34], where the aperiodic trend is assumed to correspond to the SCL, and the residual is assumed to correspond to SCRs:

$$\begin{aligned} X_{\mathrm{EDA}} &\cong \hat{X}_{\mathrm{SCL}} + \hat{X}_{\mathrm{SCR}} \\ \hat{X}_{\mathrm{SCL}} &= (1+\lambda^2 D_2^T D_2)^{-1} X_{\mathrm{EDA}} \\ \hat{X}_{\mathrm{SCR}} &= X_{\mathrm{EDA}} - \hat{X}_{\mathrm{SCL}} \end{aligned} \tag{1}$$

where X_{EDA} is the raw EDA signal, $\hat{X}_{\mathrm{SCL}}$ is the SCL trend, and $\hat{X}_{\mathrm{SCR}}$ is the SCR component. The regularization term $\lambda^2 D_2^T D_2$ biases the solution towards a smooth trend $\hat{X}_{\mathrm{SCL}}$, where I is the identity matrix, and D_2 is a discrete approximation of the 2nd derivative operator

$$D_2 = \begin{bmatrix} 1 & -2 & 1 & 0 & \dots & 0 \\ 0 & 1 & -2 & 1 & \ddots & \vdots \\ \vdots & \ddots & \ddots & \ddots & \ddots & 0 \\ 0 & \dots & 0 & 1 & -2 & 1 \end{bmatrix}. \tag{2}$$

By increasing the regularization parameter λ, the formulation allows us to generate increasingly smoother SCL components. Experimental results of the decomposition are shown in Fig. 3 for a segment containing SCRs of various amplitudes as well

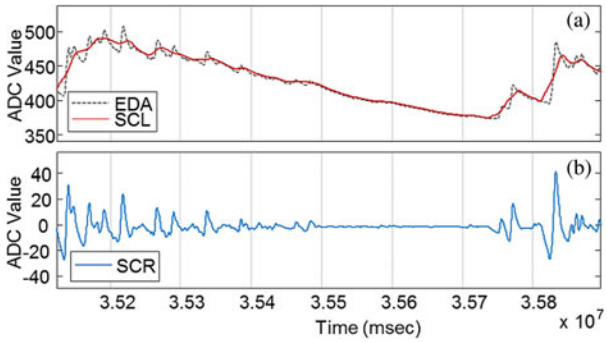

Fig. 3. Decomposition of EDA into SCL and SCR ($\lambda = 1500$).

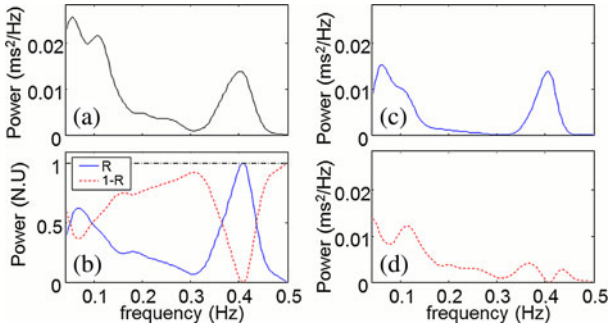

Fig. 4. Decomposition of HRV PSD into PNS-related and SNS-related components by frequency weighting according to the respiratory PSD. (a) HRV. (b) Normalized respiration. (c) PNS. (d) SNS.

as a slow decaying trend, which are the more relevant patterns in EDA; similar results were obtained across all subjects. The estimated SCL successfully captures the downward EDA trend (Fig. 3(a)), whereas the SCR component captures phasic responses at the beginning and at the end of the segment (Fig. 3(b)).

Once the EDA signal has been decomposed, we extract two features from the aperiodic trend, and one feature from the residual

$$\begin{aligned} \mu_{\mathrm{SCL}} &= \frac{1}{N}\sum_{i=1}^{N} \hat{X}_{\mathrm{SCL}}(t-i) \\ \rho_{\mathrm{SCL}} &= \rho(t, \hat{X}_{\mathrm{SCL}}) \\ \sigma_{\mathrm{SCR}} &= \left(\frac{1}{N}\sum_{i=1}^{N} \hat{X}^2_{\mathrm{SCR}}(t-i)\right)^{1/2} \end{aligned} \tag{3}$$

where t represents time and $\rho(a,b)$ represents the correlation coefficient between variables a and b; thus the feature ρ_{SCL} captures the degree of linearity of the SCL trend, which we expected would be higher during the smooth decays that are typical of relaxation phases (see Fig. 5). In turn, the feature μ_{SCL} is the average SCL trend over the past N samples and represents the tonic or baseline EDA. Finally, the feature σ_{SCR} captures the standard deviation in the residual $\hat{X}_{\mathrm{SCR}}$, which will be high in the presence of phasic EDA responses.

B. Feature Extraction from Heart Rate Variability

Spectral analysis of HRV shows two dominant frequency bands: a low-frequency component (LF; 0.04-0.15 Hz) mediated by both PNS and SNS, and a high-frequency component (HF; 0.15-0.4 Hz) mediated by PNS activation [35]. As a result, the ratio of LF to HF power is sometimes used as an index of autonomic balance [35]. However, HRV can be influenced by factors other than mental stress, and one of the most influential short-term factors is respiration. Thus, when using HRV as a measure of stress, it is critical to separate respiratory contributions to HRV from those that are due to the psychological stressors of interest.

To address this issue, we propose a spectral weighting procedure to decompose HRV into respiratory-driven and stress-driven components. Namely, we estimate the respiratory-induced HRV (PNS related) by weighting the HRV power spectral density (S_{HRV}) by the normalized respiratory power spectral density ($\tilde{S}_{\mathrm{resp}}$). Likewise, we estimate the stress-induced HRV (SNS related) as the residual power

$$\begin{aligned} S_{\mathrm{PNS}}(f) &= S_{\mathrm{HRV}}(f) \times \tilde{S}_{\mathrm{resp}}(f) \\ S_{\mathrm{SNS}}(f) &= S_{\mathrm{HRV}}(f) - S_{\mathrm{PNS}}(f) \end{aligned} \tag{4}$$

where $\tilde{S}_{\mathrm{resp}}$ is the [0, 1] normalized respiratory power spectra

$$\tilde{S}_{\mathrm{resp}}(f) = \frac{S_{\mathrm{resp}}(f) - \min(S_{\mathrm{resp}})}{\max(S_{\mathrm{resp}}) - \min(S_{\mathrm{resp}})} \tag{5}$$

where $0.04 \le f \le 0.5$ and S_{resp} is the power spectra of the raw respiratory signal. As a result, the ratio between S_{PNS} and S_{SNS} can be treated as an index of stress

$$r_{\mathrm{PNS/SNS}} = \frac{\Sigma_f S_{\mathrm{PNS}}(f)}{\Sigma_f S_{\mathrm{SNS}}(f)}. \tag{6}$$

The overall procedure is illustrated in Fig. 4. This approach is robust to noise on the respiratory signal and, unlike previous approaches [36] it does not require special calibration. In addition to the ratio $r_{\mathrm{PNS/SNS}}$, we also compute the average instantaneous heart period (AVNN) as an additional feature [35]. AVNN was chosen because it contains information about the baseline HRV, which is discarded in the HRV PSD.

C. Stress Prediction Model

The five features[2] (three from EDA, two from HRV) are used as predictor variables in a logistic regression model [37] that estimates the log ratio between the two outcomes in our experiment (i.e., stress versus no-stress) as a linear combination of the predictor variables

$$p_{\mathrm{stress}} = f(x,\beta) = \frac{1}{1 + e^{-(\beta_0 + \beta_1 x_1 + \cdots + \beta_k x_k)}} \tag{7}$$

where p_{stress} is the probability of stress, and x is a vector of predictor variables ($k = 5$). Each regression coefficient describes the contribution of each feature to the dependent variable (β_0 is an intercept). A positive coefficient indicates that a feature increases the probability of the event (stress), whereas a negative coefficient indicates that a feature decreases the probability

[2]Information from the EMG sensor is not included in this study since the experimental protocol (described in section V) focused on short-term stressors.

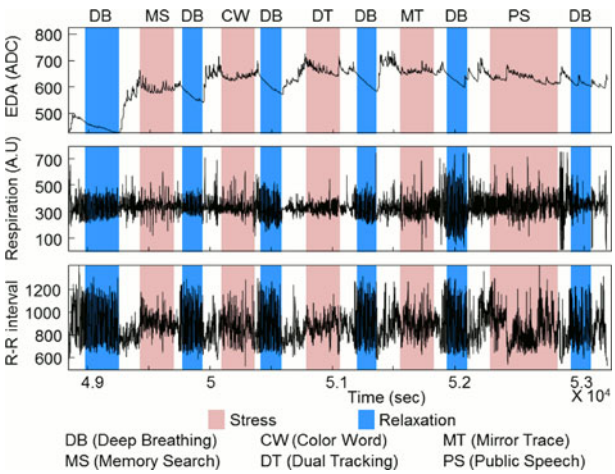

Fig. 5. EDA, respiration and HRV signals for one of the subjects (#5).

of the event. We estimate these coefficients following the maximum likelihood criterion by means of iteratively reweighted least squares (IRLS) [38]. IRLS is used to find the maximum likelihood estimates of the generalized linear model

$$L(X,\beta) = \sum_i (y_i \ln(f(x_i,\beta)) + 1(1-y_i)\ln(1-f(x_i,\beta))$$

$$\hat{\beta} = \arg\max_{\beta} L(X,\beta) \tag{8}$$

where $y_i = \{0,1\}$ is a stress indicator variable for the ith event in a training set ($y_i = 1$ if stress; $y_i = 0$ otherwise). Because the performance of the logistic regression model can be evaluated on the basis of the maximum log likelihood for a set of features, we employ a forward feature selection procedure with a likelihood-ratio test to identify a reduced set of features that provide the best performance.

V. Experimental Protocol

To assess the effectiveness of the wearable sensor system, feature-selection procedures, and prediction model, we collected experimental data from two experimental conditions[3]: mental stress and relaxation. The mental stress condition consisted of a battery of tests: dual tracking, memory search, mirror tracing, Stroop color word test, and public speech [39], whereas the relaxation condition consisted of deep breathing exercises.

1) Dual tracking: Subjects had to track a moving target in a computer screen using a mouse, and left-click whenever one of three target letters appeared on the screen (5 min).
2) Memory search: Ss were told to memorize a set of words presented in sequence, and then recognize them among a number of confounders under time pressure (5 min).
3) Mirror tracing: Ss had to manually trace a pattern on a paper printout by looking through a mirror (5 min).
4) Stroop: Ss were shown one of four words (red, green, blue, yellow) displayed in different ink colors, and had to click on one of four buttons according to the ink color (5 min).
5) Public speech: Ss were asked to prepare a short speech on a current topic (3 min), deliver the speech to an audience (4 min), and address questions (3 min).
6) Relaxation: Ss were asked to breathe deeply at a pace of 0.1 Hz (breathe in for 4 s, breathe out for 6 s.) (3 min).

The tests were performed according to the sequence deep breathing (DB), memory search, DB, color word test, DB, dual task, DB, mirror trace, DB, public speech, and DB. We interleaved deep breathing between stress tests to allow subjects to recover between consecutive stressors. We collected data from ten subjects. Subjects rated their perceived stress levels on a 7-point Likert scale at the end of each task.

[3]The experimental protocol was approved by the Institutional Review Board at Texas A&M University; all subjects provided written informed consent for the study. All subjects were examined and received checkup by a medical doctor for health and chronic stress.

VI. Results

Raw EDA, RR tachogram, and respiratory signals for one of the subjects are shown in Fig. 5. The respiratory signal, which is regular and of high amplitude during deep breathing exercises, becomes irregular during the stress segments. The EDA shows a decaying SCL trend during deep breathing and distinct SCR peaks during the stress segments. Finally, the RR interval becomes large (low heart rate) during relaxation and short during the stressors.

To validate the wearable sensor system and our choice of stress-related features, we formed a binary classification problem where the goal was to discriminate between the five mental stress conditions (dual tracking, memory search, mirror tracing, Stroop, and public speech) and the relaxation condition (deep breathing). EDA and HRV features (described in Section IV) were calculated using 90 s windows with an overlap of 80 s. For each subject, the respective five features were normalized to have zero mean and unit standard deviation. As described in Section IV.C, we performed a forward feature selection using the logistic regression to find a set of optimized features. Results are summarized in Fig. 6. The PNS/SNS ratio shows the largest beta coefficient and negative polarity, as increases in PNS/SNS ratio are indicative of relaxation. SCR (standard deviation of the EDA residual) shows the second highest beta coefficient but positive polarity, as SCRs increase with stress. Using a two-sided t-test (H_0: *coefficient* $\beta_i = 0$), all five coefficients are significant at the $p = 0.0001$ level. For the final model, however, variable ρ_{SCL} was not selected since its coefficient (-0.02) was significantly smaller than for other variables (μ_{SCL}: 0.81; σ_{SCR}: 1.14; $r_{\mathrm{PNS/SNS}}$: -1.2; $AVNN$: -0.9). This indicates that ρ_{SCL} has no significant diagnostic value when compared to the other predictor variables.

We tested the predictive accuracy of the logistic regression model in a leave-one-subject-out fashion, where nine subjects were selected for training and the remaining subject was used for testing. For each combination of training and test sets (ten different splits), the logistic regression model was estimated from training data and then used to estimate the probability p_{stress} for samples in the test set. Next, we used the threshold $p_{\mathrm{stress}} \geq 0.5$ as the decision boundary to label an event as stressful.

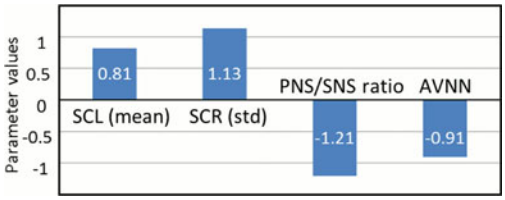

Fig. 6. Optimized logistic regression coefficients. Four features are chosen from a forward feature selection procedure.

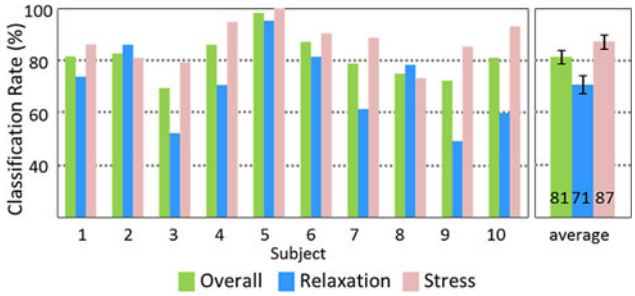

Fig. 7. Classification result using logistic regression. Mean SCL, standard deviation of SCR, PNS/SNS ratio, and AVNN were chosen as features in a forward feature selection procedure.

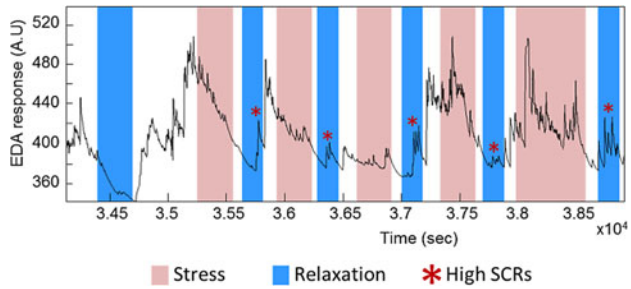

Fig. 8. EDA for Subject 9 shows strong SCRs during the relaxation segments.

Classification performance was averaged across the ten splits; results are summarized in Fig. 7. The average classification rate using the four features in Fig. 6 is 0.81, with a true positive rate of 0.87, and a true negative rate of 0.71; classification rates remain unchanged if ρ_{SCL} is added to the logistic regression model.

As shown in Fig. 7, the logistic regression model has a true negative rate close to chance level (0.50) for several subjects (e.g., #3 and #9). Close inspection of the EDA response for these subjects reveals the presence of strong SCRs during the deep breathing exercise (see Fig. 8), which suggests that the subjects were unable to relax during these exercises. In fact, subjective ratings collected after the experiment show that the subject #9 rated the deep breathing exercise as highly stressful. These results illustrate the inherent difficulty of the problem, both in terms of designing stress and relaxation elicitation protocols, and in terms of taking these labels at face value.

VII. Discussion and Conclusion

We have designed and developed a minimally-invasive wearable sensor platform which allows long-term ambulatory monitoring of a number of physiological indicators of mental stress. Our design is a concerted effort to balance information content and comfort. The system consists of a number of selected wireless sensors (EDA, respiration, HRM, and EMG) that communicate with a holster unit by means of a lightweight communication protocol. The system weighs 277 grams (holster and wireless sensors), and allows uninterrupted operation in excess of 13 hours. The system was validated through a series of tests that elicited mental stress and relaxation. Stress-related features were obtained from EDA, HRM, and respiration sensors. Using a logistic regression model, our feature set can predict the presence of stress with an accuracy of 0.81.

Our experimental results show promise for the monitoring of mental stress during daily activities of subjects. First, our method can combine information from multiple physiological signals into a single index of stress which, by virtue of the logistic regression model, remains interpretable. In the process, we have proposed a robust and computationally simple analysis method that is able to decouple respiratory and stress influences in heart rate variability. Results from logistic regression indicate that this HRV index has the highest predictive power, closely followed by the skin conductance response (SCR).

Several improvements to the hardware system are being undertaken at the time of this writing. First, we are developing an android-based platform to serve as a graphical user interface for the sensor system. This addition will allow a user to observe their physiological signals in real time, manage the operation of the device, monitor the status of the sensors, and also provide useful metadata (e.g., subjective ratings of stress, activities). Presently, the respiratory and EDA sensor module requires careful manual calibration (offset and gain potentiometers) at the beginning of each experimental session. To address this issue, we are designing an autocalibration circuit that replaces each potentiometer with a programmable resistor (an R-2R ladder combined with an analog multiplexer) controlled by the MSP430 microcontroller, so that both values can be adjusted (and recorded) in real time. This improvement will minimize the time-consuming manual calibration stage and allow inexperienced users to use the sensor without any assistance from the experimenter.

Acknowledgment

Le Zhang and Muna Sheet are greatly acknowledged for their help with building wireless nodes and conducting experiments. Professor Joydeep Ghosh is also gratefully acknowledged for suggesting the use of logistic regression as the stress prediction model. The authors are thankful to Daniel Felps and Folami Alamudun for their assistance with editing this manuscript.

References

[1] H. Selye, *The Stress of Life*, 2nd ed. New York: The McGraw-Hill Companies, 1978.

[2] L. O. Jimenez and D. A. Landgrebe, "Supervised classification in high-dimensional space: Geometrical, statistical, and asymptotical properties of multivariate data," *IEEE Trans. Syst. Man Cybern. Part C*, vol. 28, no. 1, pp. 39–54, Feb. 1998.

[3] F. Gemperle, C. Kasabach, J. Stivoric, M. Bauer, and R. Martin, "Design for wearability," in *Proc. Int. Symp. Wearable Comput.*, Pittsburgh, PA, 1998, pp. 116–122.

[4] S. Kasl, "Stress and health," *Annu. Rev. Public Health*, vol. 5, pp. 319–341, 1984.
[5] S. Cobb and R. Rose, "Hypertension, peptic ulcer, and diabetes in air traffic controllers," *J. mer.College Cardiology*, vol. 224, p. 489, 1973.
[6] K. Raikkonen, R. Lassila, L. Keltikangas-Jarvinen, and A. Hautanen, "Association of chronic stress with plasminogen activator inhibitor–1 in healthy middle-aged men," *Arteriosclerosis, Thrombosis, Vascular Biol.*, vol. 16, pp. 363–367, 1996.
[7] N. R. Carlson, *Physiology of Behavior*, 10th ed. Needham Heights, MA: Allyn and Bacon, 2009.
[8] B. Takkouche, C. Regueira, and J. Gestal-Otero, "A cohort study of stress and the common cold," *Epidemiology*, vol. 12, pp. 345–349, 2001.
[9] B. McEwen, "Protective and damaging effects of stress mediators," *The New England J. Med.*, vol. 338, p. 171, 1998.
[10] S. Cohen, D. Tyrrell, and A. Smith, "Negative life events, perceived stress, negative affect, and susceptibility to the common cold," *J. Personality Soc. Psychol.*, vol. 64, pp. 131–140, 1993.
[11] A. Luneski, E. Konstantinidis, and P. Bamidis, "Affective medicine: A review of affective computing efforts in medical informatics," *Methods Inf. Med.*, vol. 49, pp. 207–218, 2010.
[12] J. Kim and E. André, "Emotion recognition based on physiological changes in music listening," *IEEE Trans. Pattern Anal. Mach. Intell.*, vol. 30, no. 12, pp. 2067–2083, Dec. 2008.
[13] R. L. Mandryk and M. S. Atkins, "A fuzzy physiological approach for continuously modeling emotion during interaction with play technologies," *Int. J. Human Comput. Stud.*, vol. 65, pp. 329–347, 2007.
[14] F. Nasoz, C. Lisetti, and A. Vasilakos, "Affectively intelligent and adaptive car interfaces," *Inf. Sci.*, vol. 180, pp. 3817–3836, 2010.
[15] B. Arnrich, C. Setz, R. La Marca, G. Troster, and U. Ehlert, "What does your chair know about your stress level?" *IEEE Trans. Inf. Technol. Biomed.*, vol. 14, no. 2, pp. 207–214, Mar. 2010.
[16] C. Lisetti, F. Nasoz, C. LeRouge, O. Ozyer, and K. Alvarez, "Developing multimodal intelligent affective interfaces for tele-home health care," *Int. J. Human Comput. Stud.*, vol. 59, pp. 245–255, 2003.
[17] T. Vrijkotte, L. van Doornen, and E. de Geus, "Effects of work stress on ambulatory blood pressure, heart rate, and heart rate variability," *Hypertension*, vol. 35, pp. 880–886, 2000.
[18] R. Fensli, P. Pedersen, T. Gundersen, and O. Hejlesen, "Sensor acceptance model–measuring patient acceptance of wearable sensors," *Methods Inf. Med.*, vol. 47, pp. 89–95, 2008.
[19] M. E. Dawson, A. M. Schell, and D. L. Filion, "The electrodermal system," in *Handbook of Psychophysiology*, 3rd ed. Cambridge, U.K.: Cambridge Univ. Press, 2007.
[20] U. Lundberg, R. Kadefors, B. Melin, G. Palmerud, P. Hassmen, M. Engstrom, and I. Dohns, "Psychophysiological stress and EMG activity of the trapezius muscle," *Int. J. Behav. Med.*, vol. 1, pp. 354–370, 1994.
[21] R. DeVaul, M. Sung, J. Gips, and A. Pentland, "MIThril 2003: Applications and architecture," in *Proc. Int. Symp. Wearable Comput.*, White Plains, NY, 2003, pp. 4–11.
[22] M. Pacelli, G. Loriga, N. Taccini, and R. Paradiso, "Sensing fabrics for monitoring physiological and biomechanical variables: e-textile solutions," in *Proc. IEEE/EMBS Int. Summer School Med. Devices Biosensors*, Cambridge, MA, Sep. 4–6, 2006, pp. 1–4.
[23] U. Anliker, J. Ward, P. Lukowicz, G. Troster, F. Dolveck, M. Baer, F. Keita, E. Schenker, F. Catarsi, and L. Coluccini, "AMON: a wearable multiparameter medical monitoring and alert system," *IEEE Trans. Inf. Technol. Biomed.*, vol. 8, no. 4, pp. 415–427, Dec. 2004.
[24] C. Mundt, K. Montgomery, U. Udoh, V. Barker, G. Thonier, A. Tellier, R. Ricks, R. Darling, Y. Cagle, and N. Cabrol, "A multiparameter wearable physiologic monitoring system for space and terrestrial applications," *IEEE Trans. Inf. Technol. Biomed.*, vol. 9, pp. 382–391, 2005.
[25] V. Shnayder, B. Chen, K. Lorincz, T. Fulford-Jones, and M. Welsh, "Sensor networks for medical care,", Technical Report TR-08-05, Div. of Engineering and Applied Sciences, Harvard University, 2005.
[26] E. Monton, J. Hernandez, J. Blasco, T. Herve, J. Micallef, I. Grech, A. Brincat, and V. Traver, "Body area network for wireless patient monitoring," *IET Communications*, vol. 2, pp. 215–222, 2008.
[27] A. Sahakian, W. Tompkins, and J. Webster, "Electrode motion artifacts in electrical impedance pneumography," *IEEE Trans. Biomed. Eng.*, vol. BME 32, no. 6, pp. 448–451, 1985.
[28] G. Brüllmann, K. Fritsch, R. Thurnheer, and K. Bloch, "Respiratory monitoring by inductive plethysmography in unrestrained subjects using position sensor-adjusted calibration," *Respiration*, vol. 79, pp. 112–120, 2009.
[29] M. El-Sheikh, "The role of emotional responses and physiological reactivity in the marital conflict–child functioning link," *J. Child Psychol. Psychiatry*, vol. 46, pp. 1191–1199, 2005.
[30] C. L. Lim, C. Rennie, R. J. Barry, H. Bahramali, I. Lazzaro, B. Manor, and E. Gordon, "Decomposing skin conductance into tonic and phasic components," *Int. J. Psychophysiol.*, vol. 25, pp. 97–109, 1997.
[31] D. Alexander, C. Trengove, P. Johnston, T. Cooper, J. August, and E. Gordon, "Separating individual skin conductance responses in a short interstimulus-interval paradigm," *J. Neurosci. Methods*, vol. 146, pp. 116–123, 2005.
[32] M. Benedek and C. Kaernbach, "Decomposition of skin conductance data by means of nonnegative deconvolution," *Psychophysiology*, vol. 47, pp. 647–658, 2010.
[33] C. Frantzidis, E. Konstantinidis, C. Pappas, and P. Bamidis, "An automated system for processing electrodermal activity," *Studies Health Technol. Informatics*, vol. 150, p. 787, 2009.
[34] M. P. Tarvainen, P. O. Ranta-aho, and P. A. Karjalainen, "An advanced detrending method with application to HRV analysis," *IEEE Trans. Biomed. Eng.*, vol. 49, pp. 172–175, 2002.
[35] M. Malik, A. J. Camm, J. J. Thomas Bigger, G. Breithardt, Sergio Cerutti, R. J. Cohen, P. Coumel, E. L. Fallen, H. L. Kennedy, R. E. Kleiger, F. Lombardi, A. Malliani, A. J. Moss, J. N. Rottman, Georg Schmidt, P. J. Schwartz, and D. H. Singer, "Heart rate variability: Standards of measurement, physiological interpretation and clinical use," *Circulation*, vol. 93, pp. 1043–1065, 1996.
[36] J. Choi and R. Gutierrez-Osuna, "Estimating mental stress using a wearable cardio-respiratory sensor," in *Proc. IEEE Sensors 2010 Conf.*, Waikoloa, HI, pp. 150–154.
[37] R. Edelberg, "Electrical properties of the skin," *Methods Psychophysiol.*, pp. 1–53, 1967.
[38] P. Rani, N. Sarkar, and C. Liu, "Maintaining optimal challenge in computer games through real-time physiological feedback," in *Proc. Int. Conf. Human Comput.*, Las Vegas, NV, 2005, pp. 184–192.
[39] D. Reeves, S. LaCour, K. Winter, K. Raynsford, and K. Vogel, The UTC-PAB/AGARD STRES Battery: User's manual and system documentation. Pensacola, FL: Naval Aerospace Medical Research Laboratory, 1991.

Jongyoon Choi (S'10) received the B.S. degree in industrial engineering from the Sunfkyunkwan University, Seoul, Korea, in 1995, and the M.S. degrees in computer engineering from Gwangju Institute of Science and Technology, Gwangju, Korea, in 1998. He is currently working toward the Ph.D. degree at Texas A&M University, College Station, TX.

His research interests include pattern recognition, affective computing, wearable sensors, and psychophysiology.

Beena Ahmed (M'04) received the B.Eng degree from the University of Engineering and Technology, Lahore, Pakistan, in 1993, and the Ph.D. degree from the University of New South Wales, Sydney, Australia, in 2004, both in electrical engineering.

She is currently a Lecturer at the Texas A&M University at Qatar, Doha, Qatar. She was a Postdoctoral Fellow with the RMIT University, Melbourne, Australia, until 2005. Her research interests include biomedical signal processing, physiological stress modeling, speech processing, feature extraction, noise reduction, EEG processing, and sleep analysis.

Ricardo Gutierrez-Osuna (M'00–SM'08) received the B.S. degree in electrical engineering from the Polytechnic University, Madrid, Spain, in 1992, and M.S. and Ph.D. degrees in computer engineering from North Carolina State University, Raleigh, NC, in 1995 and 1998, respectively.

He is currently an Associate Professor of computer engineering at Texas A&M University, College Station, TX. His current research interests include wearable physiological sensors, voice and accent conversion, speech and face perception, and active chemical sensing.